1 **Sources and sinks driving sulphuric acid concentrations in contrasting environments:**
2 **implications on proxy calculations**

4 Lubna Dada[1,2], Ilona Ylivinkka[2,3], Rima Baalbaki[2], Chang Li[1], Yishuo Guo[1], Chao Yan[1,2], Lei Yao[1,2],
5 Nina Sarnela[2], Tuija Jokinen[2], Kaspar R. Daellenbach[2], Rujing Yin[4], Chenjuan Deng[4], Biwu Chu[1,2],
6 Tuomo Nieminen[2], Jenni Kontkanen[2], Dominik Stolzenburg[2], Mikko Sipilä[2], Tareq Hussein[2], Pauli
7 Paasonen[2], Federico Bianchi[2], Imre Salma[5], Tamás Weidinger[6], Michael Pikridas[7], Jean Sciare[7],
8 Jingkun Jiang[4], Yongchun Liu[1], Tuukka Petäjä[2], Veli-Matti Kerminen[2], Markku Kulmala[1,2]

10 [1] Aerosol and Haze Laboratory, Beijing Advanced Innovation Center for Soft Matter Science and Engineering, Beijing
11 University of Chemical Technology, Beijing, China.
12 [2] Institute for Atmospheric and Earth System Research INAR / Physics, Faculty of Science, University of Helsinki,
13 Finland
14 [3] SMEAR II station, University of Helsinki, 35500 Korkeakoski, Finland
15 [4] State Key Joint Laboratory of Environment Simulation and Pollution Control, School of Environment, Tsinghua
16 University, 100084 Beijing
17 [5] Institute of Chemistry, Eötvös University, 1518 Budapest, P.O. Box 32, Hungary
18 [6] Department of Meteorology, Eötvös University, H-1518 Budapest, P.O. Box 32, Hungary
19 [7] The Cyprus Institute, Climate & Atmosphere Research Centre (CARE-C), 20 Konstantinou Kavafi Street, 2121, Nicosia,
20 Cyprus

22 *Correspondence to: markku.kulmala@helsinki.fi*

24 **Abstract**
25

26 Sulphuric acid has been shown to be a key driver for new particle formation and subsequent growth
27 in various environments mainly due to its low volatility. However, direct measurements of gas-phase
28 sulphuric acid are oftentimes not available, and the current sulphuric acid proxies cannot predict for
29 example its nighttime concentrations or result in significant discrepancies with measured values.
30 Here, we define the sources and sinks of sulphuric acid in different environments and derive a new
31 physical proxy for sulphuric acid to be utilized in locations and during periods when it is not
32 measured. We used H_2SO_4 measurements from four different locations: Hyytiälä, Finland; Agia
33 Marina, Cyprus; Budapest, Hungary; and Beijing, China, representing semi-pristine boreal forest,
34 rural environment in the Mediterranean area, urban environment and heavily polluted megacity,
35 respectively. The new proxy takes into account the formation of sulphuric acid from SO_2 via OH
36 oxidation and other oxidation pathways, specifically that via stabilized Criegee Intermediates. The
37 sulphuric acid sinks included in the proxy are its condensation sink (CS) and atmospheric clustering
38 starting from H_2SO_4 dimer formation. Indeed, we found that the observed sulphuric acid
39 concentration can be explained by the proposed sources and sinks with similar coefficients in the four
40 contrasting environments where we have tested it. Thus, the new proxy is a more flexible and an
41 important improvement of previous proxies. Following the recommendations in the manuscript, a
42 proxy for a specific location can be derived.

43

44 Keywords: sulphuric acid, proxy, boreal, rural, urban, megacity
45

1. Introduction

Atmospheric New Particle formation (NPF) events and their subsequent growth have been observed to take place almost everywhere in the world (Kulmala et al., 2004; Kerminen et al., 2018; Chu et al., 2019). Many of these observations are based on continuous measurements and some include more than a year of measurement data (Nieminen et al., 2018). The importance of NPF events on the global aerosol budget and cloud condensation nuclei formation has been well established (Spracklen et al., 2008; Merikanto et al., 2009; Spracklen et al., 2010; Kerminen et al., 2012; Gordon et al., 2017). Recently, the contribution of NPF to haze formation, which was still controversial, is being investigated in an increasing number of studies from Chinese megacities (Guo et al., 2014; Zamora et al., 2019).

Sulphuric acid (H_2SO_4), which has a very low saturation vapor pressure, has been found to be the major precursor of atmospheric NPF (Weber et al., 1996; Kulmala et al., 2004; Sihto et al., 2006; Sipilä et al., 2010; Erupe et al., 2011; Lehtipalo et al., 2018; Ma et al., 2019). However, atmospheric measurements of gas-phase sulphuric acid are rare, mainly due to its low concentration (10^6–10^7 molecules cm^{-3} or below) that can only be measured using state-of-the art instruments (Mikkonen et al., 2011) such as the Chemical Ionization atmospheric pressure interface time of flight spectrometer (CI-APi-ToF) (Eisele and Tanner, 1993; Jokinen et al., 2012). Therefore, a physically and chemically sound proxy is needed to estimate H_2SO_4 concentrations in various environments where NPF events are observed but H_2SO_4 concentrations are not continuously measured.

Due to its important participation in clustering and thus in the NPF process, several studies have tried to produce proxies for H_2SO_4 in order to fill gaps in data. For example, Petäjä et al. (2009) developed an approximation of gas-phase H_2SO_4 concentration in Hyytiälä, southern Finland, using its source from reactions between SO_2 and OH radicals, and its loss by condensation onto pre-existing particles (condensation sink, CS). Later, Mikkonen et al. (2011) developed H_2SO_4 proxies based on measurements at six urban, rural and forest areas in European and North American sites. Proxies developed by Mikkonen et al. (2011) suggested that the sulphuric acid concentration depends mostly on the available radiation and SO_2 concentration, with little influence by CS. However, Lu et al. (2019), who developed a daytime proxy based on measurement in Beijing China, proved the need of taking into account the CS when approximating gaseous H_2SO_4, especially in areas where the condensational sink can be relatively high. The proxy developed by Lu et al. (2019) takes into consideration the formation pathways of H_2SO_4 via OH radicals from both the conventional photolysis of O_3 and from the photolysis of HONO, as well as, the loss of H_2SO_4 via CS.

Here, we derive a new proxy which takes into account the production of gaseous sulphuric acid from SO_2 with oxidation by OH and stabilized Criegee Intermediates (Mauldin et al., 2012) reactions, and its losses onto pre-existing aerosol particles (condensation sink) and due to molecular cluster formation. In order to evaluate the accuracy of the our hypothesized sources and sinks and the goodness of our new proxy, we utilize measurements from four different locations: (1) Hyytiälä, Finland, (2) Agia Marina, Cyprus, (3) Budapest, Hungary and (4) Beijing, China, representing a semi-pristine boreal forest environment, rural environment in the Mediterranean area, urban environment and heavily polluted megacity, respectively. We further compare the coefficients of production and losses in each environment in order to understand the prevailing mechanism of the H_2SO_4 budget in each of the studied environments. As a result of this investigation, a well-defined sulphuric acid

92 concentration can be derived for multiple areas around the world and even extended in time during
93 times when it was not measured (such as: gap filling, forecast, prediction, estimation, etc.).
94
95 **2. Measurement locations, observations and instrumentation**
96
97 2.1. **Locations**
98 **Semi-pristine boreal forest environment: Hyytiälä, Finland**
99
100 Measurements were conducted at the SMEAR II-station, located in Hyytiälä (61.1° N, 24.17°E, 181
101 m a.s.l. (Hari and Kulmala, 2005)), southern Finland. Here we used measurements from August 18,
102 2016 to April 16, 2017 and from March 8, 2018 to February 28, 2019. The measurements were
103 performed at a tower 35 m above the ground level. A summary for all locations and instrumentation
104 is given in Table S1.
105
106 **Rural background site: Agia Marina, Cyprus**
107
108 Measurements were conducted at the Cyprus Atmospheric Observatory (CAO) (35.03 N, 33.05° E;
109 532 m a.s.l.), a rural background site located close to Agia Marina Xyliatou village, between February
110 22 and March 3, 2018. For more details, see for example Pikridas et al. (2018).
111
112 **Urban location: Budapest, Hungary**
113
114 The measurements took place at the Budapest platform for Aerosol Research Training (BpART)
115 Research Laboratory (N 47° 28' 30'', E 19° 03' 45'', 115 m a.s.l.) of the Eötvös University situated on
116 the bank of the Danube between March 21 and May 2, 2018. The site represents a well-mixed average
117 atmosphere of the city centre Salma et al. (2016).
118
119 **Polluted megacity: Beijing, China**
120
121 Here the observations were performed during December 1, 2018 to January 31, 2019, at the west
122 campus of Beijing University of Chemical Technology (39.94° N, 116.30° E). The sampling took
123 place from outside the window at the 5th floor of a university building adjacent to a busy street. For
124 more details, see for example Lu et al. (2019); Zhou et al. (2020).
125
126 2.2. **Instrumentation**
127
128 **Trace Gases**
129
130 A summary for all locations and instrumentation is given in Table S1. In all four locations, the
131 sulphuric acid concentrations were measured using a Chemical Ionization atmospheric pressure
132 interface time of flight spectrometer (CI-APi-ToF) (Eisele and Tanner, 1993; Jokinen et al., 2012)
133 with NO_3^- as a reagent ion and analyzed using a tofTools package based on MATLAB software
134 (Junninen et al., 2010). In Hyytiälä and Beijing, the SO_2 and O_3 concentrations were measured using
135 an SO_2 analyzer (Model 43i, Thermo, USA), with a detection limit of 0.1 ppbv, and O_3 analyzer
136 (Model 49i, Thermo, USA), respectively. In Cyprus, SO_2 and O_3 are monitored using Ecotech
137 Instruments (9850 and 9810, respectively). Concentrations of SO_2 in Budapest were measured by UV

138 fluorescence (Ysselbach 43C) with a time resolution of 1 h at a regular station of the National Air
139 Quality Network located in 1.7 km in the upwind prevailing direction from the BpART site. It was
140 shown earlier that the hourly average SO_2 concentrations (See Figure S1) in central Budapest are
141 ordinarily distributed without larger spatial gradients (Salma and Németh, 2019).
142
143 **Particle number Size Distribution**
144
145 The condensation sink (CS) was calculated using the method proposed by Kulmala et al. (2012) from
146 number size distribution measurements. In Hyytiälä, the particle number size distribution was
147 measured using a twin differential mobility particle sizer (DMPS) (Aalto et al., 2001). Hygroscopic
148 growth correction (Laakso et al., 2004) was included when calculating the CS in Hyytiälä (Figure
149 S2). In Agia Marina, the particle number size distribution between 2 and 800 nm was reconstructed
150 from two instruments: an Airel NAIS (Neutral cluster and Air Ion Spectrometer, 2-20 nm) and TSI
151 SMPS (Scanning Mobility Particle Sizer, 20-800 nm). In Budapest, the particle number size
152 distributions were measured by a flow-switching type DMPS in a diameter range from 6 to 1000 nm
153 in the dry state of particles (RH<30%) in 30 channels with a time resolution of 8 min (Salma et al.,
154 2016b). In Beijing, the particle number size distribution between 3 nm and 850 nm was measured
155 using a Particle Size Distribution System (PSD,(Liu et al., 2016)).
156
157 **Radiation**
158
159 In Hyytiälä, Global radiation (GlobRad) was measured using a SK08 solar pyranometer until August
160 24, 2017 and after that using a EQ08-S solar pyranometer. The measurements were relocated from
161 18-m height to 37-m height on February 14, 2017. Global Radiation from the Agia Marina is
162 monitored using a weather station (Campbell Scientific Europe). In Budapest, global radiation was
163 measured by an SMP3 pyranometer (Kipp and Zonnen, The Netherlands) on the roof of the building
164 complex with a time resolution of 1 min. Its operation was checked by comparing the measured data
165 with those obtained from regular radiation measurements performed by a CMP11 pyranometer (Kipp
166 and Zonnen, The Netherlands) at the Hungarian Meteorological Service (HMS) in a distance of 10
167 km. The annual mean GlobRad ratio and SD of the 1-h values for the BpART and HMS stations were
168 1.03±0.23 for GlobRad > 100 W m^{-2}, which changed to 1.01±0.05 when considering additionally
169 clear sky conditions. In Beijing, GlobRad intensity was measured at the rooftop of the 5-floor building
170 using a Vaisala Weather station data acquisition system (AWS310, PWD22, CL51), Metcon.
171
172 **Alkenes**
173
174 Volatile organic compounds (VOCs) were measured with a proton transfer reaction quadrupole mass
175 spectrometer (PTR-MS, Ionicon Analytik GmbH) in Hyytiälä. Ambient mixing ratios are measured
176 every third hour from several different measurement heights. In this study, we use data from 16.8 m
177 height. The instrument is calibrated regularly with standard gas (Apel-Riemer Environmental, Inc.)
178 (Taipale et al., 2008).
179 In Beijing, VOCs were measured using single photon ionization time-of-flight mass spectrometer
180 (SPI-MS 3000R, Hexin Mass Spectrometry) with unit mass resolution (UMR) (Gao et al., 2013) from
181 September 27, 2018 and May 28, 2019. The alkenes included here are propylene, butylene, butadiene,
182 isoprene, pentene and hexene. As the instrument cannot distinguish conformers, the pentene and

183   hexene could also be cyclopentene and cyclohexene. Correlation coefficients between the different
184   variables used in our study in all four locations are shown in Figures S3-S7.

185

186   **3.   Derivation of the new proxy**

187

188   We applied the following equation to describe the time-evolution of gas-phase sulphuric acid
189   concentration:

190

191   $\frac{d[H_2SO_4]}{dt} = k_0[OH][SO_2] + k_2[O_3][Alkene][SO_2] - CS[H_2SO_4] - k_3[H_2SO_4]^2$ (1)

192

193   Here, k_o represents the coefficient of H_2SO_4 production term due to the well-known SO_2 - OH reaction
194   (Petäjä et al., 2009) and k_2 is the coefficient of H_2SO_4 production via stabilized Criegee Intermediates
195   (sCI) produced by the ozonolysis of alkenes (Mauldin et al., 2012). Here we use available
196   monoterpene concentration (MT) as a proxy for alkenes in Hyytiälä as they are the dominating species
197   in the boreal forest environment (Hakola et al., 2012; Hellén et al., 2018; Rinne et al., 2005). For
198   Beijing, we use urban dominating aromatic alkenes. As no VOC measurements are performed in
199   neither Agia Marina nor Budapest, we evaluate the proxy without the stabilized Criegee Intermediate
200   source term. It is important to note here that the coefficient for sCI is a "bulk" term, and it varies from
201   place to place due to the differences in sCI structures and different production efficiency from
202   different alkene species (Novelli et al., 2017; Sipilä et al., 2014). The third term in Equation 1
203   represents the loss of H_2SO_4 to pre-existing aerosol particles, known as condensation sink (CS). The
204   fourth term in Equation 1 takes into account the additional loss of H_2SO_4 due to cluster formation not
205   included in the term containing CS. This is necessary because CS is only inferred from size-
206   distribution measurements at maximum down to 1.5 nm, i.e. not containing any cluster concentrations
207   and hence losses onto these clusters. This term is written in the form of sulphuric acid dimer
208   production, which seems to be the first step of cluster formation once stabilized by bases (Kulmala et
209   al., 2013; Almeida et al., 2013; Yao et al., 2018).

210

211   Since measuring the OH concentration is challenging, we first replaced it with the UVB radiation
212   intensity, which has been shown to be a good proxy for the OH concentration (Berresheim et al.,
213   2002; Lu et al., 2019; Rohrer and Berresheim, 2006). Unfortunately, UVB was not measured in all
214   the field studies considered here. Alternatively, GlobRad, a commonly measured quantity, tends to
215   correlate well with UVB and can generally replace it, as used previously by Petäjä et al. (2009). We
216   confirmed the strong correlation between UVB radiation and Global radiation in two locations,
217   Hyytiälä and Beijing (Figure S8-S9). Accordingly, the coefficient k_1 here replaces the coefficient of
218   H_2SO_4 production k_o terms (Equation 2). We proceed here using only GlobRad in the proxy to be
219   consistent with the two other locations where UVB was not measured (Agia Marina and Budapest).

220

221

222   $\frac{d[H_2SO_4]}{dt} = k_1 GlobRad[SO_2] + k_2[O_3][Alkene][SO_2] - CS[H_2SO_4] - k_3[H_2SO_4]^2$ (2)

223

224

225   By assuming a steady state between H_2SO_4 production and loss, the H_2SO_4 concentration can be
226   solved directly from Equation (2):

227

228
$$[H_2SO_4] = -\frac{CS}{2k_3} + \sqrt{\left(\frac{CS}{2k_3}\right)^2 + \frac{[SO_2]}{k_3}(k_1 GlobRad + k_2[O_3][Alkene])}$$ *(3)*

229

230 In order to evaluate the importance of each of the source terms in determining the change in sulphuric
231 acid concentration, we refitted the data after excluding the stabilized Criegee intermediates source
232 pathway as shown in Equation 4.

233

234   $$\frac{d[H_2SO_4]}{dt} = k_1 GlobRad[SO_2] - CS[H_2SO_4] - k_3[H_2SO_4]^2$$ *(4)*

235

236 In order to evaluate the importance of each of the sink terms in determining the sulphuric acid
237 concentration, we refitted the data after excluding the loss of sulphuric acid via the cluster formation
238 pathway using Equation 5.

239

240   $$\frac{d[H_2SO_4]}{dt} = k_1 GlobRad[SO_2] + k_2[O_3][Alkene][SO_2] - CS[H_2SO_4]$$ *(5)*

241

242 we also refitted the data using the simple proxy proposed by Petäjä et al. (2009) by excluding the
243 formation of sulphuric acid via stabilized Criegee intermediates source pathway and loss of sulphuric
244 acid via the cluster formation pathway using Equation 6 and evaluated it by comparing to the original
245 proxy.

246

247   $$\frac{d[H_2SO_4]}{dt} = k_1 GlobRad[SO_2] - CS[H_2SO_4]$$ *(6)*

248

249   $$\frac{d[H_2SO_4]}{dt} = 1.4x\,10^7 x\,GlobRad^{-0.7}[SO_2] - CS[H_2SO_4]$$ *(See Petäjä et al. 2009)*   *(7)*

250

251 The fitting coefficients were obtained by minimizing the sum of the squared logarithm of the ratio
252 between the proxy values and measured sulphuric acid concentration using the method described by
253 Lagarias et al. (1998), a build-in function *fminsearch* of MATLAB, giving the optimal values for the
254 coefficients. The data was subject to boot strapping when getting the *k* values as a measure of accuracy
255 in terms of bias, variance, confidence intervals, or prediction error (Efron and Tibshirani, 1994). The
256 median, 25th percentile and 75th percentiles of the coefficients are shown in for all locations together
257 with the median *k* values in Table 1. Figures S3-S5 present the correlation matrix between the
258 different variables participating in H_2SO_4 formation and loss in all locations. In Beijing, the Alkenes
259 (AVOCs) have different patterns in day and night which forces us to have two separate equations for
260 daytime and nighttime. The goodness of the fit and the probability of overfitting or under-fitting was
261 evaluated using the Akaike information criterion (Figure S10), which also compares the proxies given
262 in equations 2, 4, 5 and 6. The criterion uses the sample size (number of points), the number of
263 parameters (terms in the equation) and the sum of squared estimate of errors (SSE: deviations
264 predicted from actual empirical values of data) to estimate the quality of each model, relative to each
265 of the other models and thus provides means for model selection (McElreath, 2018).

266
267

4. Results and Discussions

4.1. The sulphuric acid proxy for Hyytiälä SMEAR II station

Figure 1 shows the scatter plot between the observed H_2SO_4 concentrations and that derived by the proxy using the full Equation 2. The correlation coefficient was 0.85 (2089 data points). The data were related to 3-hour medians, as the monoterpene concentration was measured only every third hour. In Figure 1B-D, the proxy is refitted after removing one of the source or sink terms (Equations 4-6), in order to evaluate the sensitivity of the proxy to each of the terms and to show the improvement of the proxy using the additional source and sink (Figure 1A) in comparison to the simple proxy that was used by Petäjä et al. (2009) (Figure 1D). Our results show that the integration of additional terms of H_2SO_4 formation (i.e. the stabilized Criegee Intermediates) and loss (atmospheric cluster formation) gives the new proxy the ability to accurately capture the diurnal variation of the H_2SO_4 concentration, demonstrating a clear improvement over the earlier physical proxy (Petäjä et al., 2009). In Figure 1B the corresponding data are shown without the alkene term (Equation 4). The correlation is significantly weaker (0.73) than with the full equation. Even more importantly, we cannot estimate the contribution of the alkene term to the sulphuric acid concentration (Figure 2 – Fit 2) as the fit results also in an unphysical coefficient for cluster formation (Kürten et al., 2015) and the fit fails to capture the diurnal pattern during dark hours after 16:00 (Figure 2 – Fit 2). When fitting the data without the cluster source term (Equation 5), the correlation coefficient is high (Figure 1C), yet the goodness of the fit is not as good as when the cluster source term is taken into account (Figure S10).

The fit was able to reproduce the sulphuric acid concentration in such clean environment without the cluster term (Figure 2 – Fit 3), perhaps due to low concentrations of bases participating in clustering in Hyytiälä (Jen et al., 2014). Finally, the corresponding data without both the alkene source term and cluster formation source term (Equation 6, Figure 1D) shows a weaker correlation between the measured and modelled sulphuric acid concentration (0.73), but more importantly, it deviates far from the 1:1 line during both daytime and nighttime (Figure 2 – Fit 4). It is important to note here that when deriving the Petäjä proxy (Petäjä et al. 2009), the model relied on summer data between April and June 2007 which could explain the misfit with the current data from Hyytiälä which spans the whole year. In general, using all four terms in equation 2 shows improvement over all other combinations (Equations 4-6) in terms of not only correlation coefficients and accurate diurnal cycle between measured and calculated concentrations of sulphuric acid as shown in Figures 1 and 2, but also show a better goodness of the fit as shown in Figure S10 when using the AIC statistical method.

4.2. Sulphuric Acid Proxy at a Rural Site: Agia Marina, Cyprus

Since there were no direct measurements of alkenes in Agia Marina, we had to exclude the formation of H_2SO_4 in the oxidation by sCI from the proxy, and therefore we derived only the daytime H_2SO_4 proxy concentration. The correlation between the measured and proxy concentration of H_2SO_4 was 0.88 (96 data points) which proves the truthfulness of this proxy (Figure 3). However, the slope deviates from the 1-to-1 line which could be attributed to the additional formation mechanisms that we could not include with the current data. However, the addition of the cluster loss mechanism shows a noticeable improvement over the simple proxy, in Figure 3B (R = 0.80). The cluster loss term starts to become more important in this rural environment in comparison to the boreal forest, which could be due to a higher concentration of stabilizing bases in Agia Marina compared with Hyytiälä.

314   Although both fits, Equation 4 and 6, show similar diurnal patterns (Figure 4, Fits 2 and 4), the loss
315   term due to H_2SO_4 cluster formation improved the precision of the new proxy (Figures 3). According
316   to the statistical AIC method, the goodness of the fit has improved from 161 to 71, with and without
317   the clustering term, respectively, as shown in Figure S10. Also, even without the alkene term, the new
318   coefficients derived improved the proxy in comparison to Petäjä et al. (2009) Figure 4.

319

320   ### 4.3. Proxy for urban environment: Budapest, Hungary

321

322   Next we try to understand the mechanisms of sulphuric acid formation and losses in an even more
323   complex environment, such as urban Budapest (Figures 5 & 6). Since there were no direct
324   measurements of alkenes there, neither its proxies such as monoterpenes or anthropogenic volatile
325   organic compounds, we derived the sulphuric acid proxy excluding the formation due to stabilized
326   Criegee Intermediate pathway, as in Equation 4. In comparison to the simple proxy (Figure 5B; R =
327   0.49; 262 data points), the correlation between the measured and proxy concentration of H_2SO_4
328   improved with the addition of the loss term due to cluster formation, R = 0.59 (Figure 5A). The
329   correlation between measured and modelled values of sulphuric acid became weaker in Budapest in
330   comparison to Hyytiälä and Agia Marina, which could be attributed to a more complex environment,
331   and additional pathways of sulphuric acid formation and losses. Additionally, we observed a sudden
332   SO_2 concentration change in the middle of the campaign, possibly due to sudden change in local
333   meteorology and airmass transport, which could also explain the weaker correlation (See Figure S1).
334   The loss term due to H_2SO_4 dimerization improved the precision of the new proxy in comparison to
335   the simple model as well as the Petäjä et al. (2009) derivation, as shown in Figure 6. We think that
336   the overestimation in the Petäjä proxy is because of its dependence on the SO_2/CS ratio. The proxy is
337   originally derived in Hyytiälä and when we apply the same coefficients to Budapest it gives higher
338   estimated concentration compared to the measured since SO_2/CS ratio is smaller in Budapest (Figure
339   10). It is also visible from Figures 5 and 6, that the addition of the dimerization term was capable of
340   better capturing the lower H_2SO_4 concentrations in comparison to fitting the data without the
341   dimerization term. In comparison to both Hyytiälä and Agia Marina, the coefficient associated with
342   dimerization in Budapest is slightly higher, which can be attributed to the availability of a possibly
343   facilitated clustering due to higher abundance of stabilizing bases such as amines and ammonia
344   (discussed in the later section 4.5).

345

346   ### 4.4. Proxy for Megacity: Beijing, China

347

348   In megacities, in our case Beijing, the sulphuric acid concentration is particularly high during
349   nighttime, which confirms the need for determining the contribution of sources other than OH
350   (radiation) to its formation. Our observations emphasize the contribution of the alkene pathway, as
351   without considering this route we would not replicate morning hours correctly. During daytime, there
352   is enhanced dimerization and cluster formation due to the abundance of stabilizing bases (Yao et al.,
353   2018). In addition, alkenes or volatile organic compounds during daytime are different from those
354   during nighttime, which could be attributed to a different fleet composition during those times (Yang
355   et al., 2019). For that purpose, we had to divide the data for Beijing into two groups: daytime
356   (GlobRad >= 50 W/m^2) and nighttime (GlobRad<50 W/m^2). Besides, in such a complex environment,
357   sulphuric acid might originate from sources other than the ones we accounted for in our calculation,
358   for example through the hydrolysis of SO_3 formed from non-photochemical processes (Yao et al.,

359   2020, In Prep.). As a result, we derived two separate sets of equations, as shown in Table 1. Results
360   of a combined equation are shown in Figures S11 and S12.

361

362   In Figure 7, we see an improvement of the new proxy (Equation 2) in comparison to the simple proxy
363   (Equation 6) derived by Petäjä et al. (2009) as the former takes into the account the additional sources
364   and sinks of H_2SO_4 which were not considered in previous works (See also Figure S10). Introducing
365   the alkene production term improved the accuracy of the H_2SO_4 concentration slightly for daytime
366   and significantly during nighttime (Figures 7 and 8), which supports our assumption that H_2SO_4
367   formation during nighttime is driven by stabilized Criegee Intermediates. In Figure 7B we show the
368   proxy without the alkene term. Although the correlation improves, this is only because the nighttime
369   values are not captured. In Figure 9, we see the importance of all sources and sinks predicted for
370   sulphuric acid, as Fit 1 (Equation 2) predicts best the measured sulphuric acid concentration.
371   Additionally, according to the statistical AIC method, using the full equation has the least probability
372   of inaccuracy and error in estimating the sulphuric acid concentration (Figure S10). Moreover, it is
373   clear that the addition of the cluster sink term in Megacity environment is required due to it large
374   contribution as a sink for H_2SO_4 especially due to higher concentrations of stabilizing molecules, the
375   cluster mode (sub-3 nm) particle concentration, are the highest in Chinese Megacities (Zhou et al.,
376   2020).

377

378   ### 4.5. **Sensitivity of the proxy to the H_2SO_4 sources and sinks**

379

380   The variations of coefficients related to Equation 3 can be used to get insights into the general
381   chemical behavior under current atmospheric conditions, as well as into the mechanisms of sulphuric
382   acid formation and losses in various environments. The contribution of different terms in different
383   locations seem to vary significantly. The new loss term taking into account clustering starting from
384   dimer formation needs to be taken into account in all the environments in daytime. On the other hand,
385   without alkene term it is in practice impossible to get nighttime concentrations right.

386

387   In Table 1 we have presented the fitted coefficients (Equation 3) for all our sites, whereas the
388   contributions of the different terms in the balance equation are given during daytime in Figure 9 and
389   Table 2. The variability of the coefficients (Table 1), as well as the relative contributions of each term
390   to the total sulphuric acid concentration (Table 2), could give valuable information on the mechanisms
391   resulting in sulphuric acid formation and losses. At steady state (Equation 2), the sources and sinks
392   are in balance with each other during both daytime and nighttime, but there were clear differences in
393   the individual contributions. For instance, a variation in k_1 could be due to variations in OH sources
394   and sinks. Although in urban locations OH sinks are expected to be higher and therefore k_1 to be
395   lower, additional sources of OH are available in such locations, for example HONO (Zhang et al.,
396   2019). The alkene/Criegee intermediate term was found to be an important H_2SO_4 source (Figures 1,
397   2, 7 and 8), as without it we are not able predict night or morning concentrations of H_2SO_4 properly.
398   The alkene source term contributed up to almost 100% of the H_2SO_4 sources during nighttime in
399   Beijing and up to 82% of the sources during nighttime in Hyytiälä (Table 2). The alkene term is,
400   however, not only important during nighttime but also during daytime, as it contributed to the sources
401   by a median of 41% during daytime in Beijing. It is important to note here that Criegee intermediates
402   vary between locations, they also form in different yield percentages from different alkenes (Novelli
403   et al., 2017; Sipilä et al., 2014). These stabilized Criegee intermediates also react differently under
404   different environmental conditions.

405

406   The CS term had the highest contribution to the total sink in Hyytiälä. Its contribution decreased when
407   moving towards more polluted environments (Figure 10), to become in Beijing, regardless of the
408   relatively high condensation sink in Megacities (Laakso et al., 2006; Monkkonen et al., 2005;
409   Monkkonen et al., 2004; Yao et al., 2018), smaller than that of the cluster sink term. This observation
410   might be attributed to decreased effectiveness of condensation sink in more polluted environments
411   (Kulmala et al., 2017), but also to increased contribution of the clustering sink term in such
412   environments where the concentration of stabilizing bases is highest, particularly in daytime (Yao et
413   al., 2018; Yan et al., 2018). It should be noted that measurements of ammonia and similar bases are
414   rare, so their exact contribution is difficult to estimate..

415

416   5.   Conclusions and recommendations

417

418   Sulphuric acid is a key gas-phase compound linked to secondary aerosol production in the
419   atmosphere. The concentration of sulphuric acid in the gas phase is governed by source and sink
420   terms. In this paper we define the sources and sinks of H_2SO_4 and derived a physically and chemically
421   sound proxy for the sulphuric acid concentration using measurements at 4 different locations,
422   including boreal forest environment (Hyytiälä, Finland), a rural Mediterranean site (Cyprus), an urban
423   area (Budapest) and a megacity (Beijing). When describing the change in gas phase sulphuric acid
424   concentration, we took into account two source terms: 1) photochemical oxidation of sulfur dioxide
425   and 2) sulphuric acid originating from alkene and ozone reactions and associated stabilized Criegee
426   radical pathway. For the sink terms, we considered 3) the loss rate to the pre-existing aerosol described
427   by condensation sink, and 4) loss rate of sulphuric acid monomer due to clustering process.

428

429   In general, the variation in the environmental conditions and difference in concentrations of air
430   pollutants affects the coefficients derived and therefore it is important to derive location specific
431   coefficients. The derived coefficients give insights into the general chemical behavior and into the
432   mechanisms of sulphuric acid formation and losses in various environments. As improvements from
433   previously derived proxies, without the alkene H_2SO_4 formation pathway, it is in practice impossible
434   to get nighttime concentrations. On the other hand, the additional loss term taking into account
435   clustering starting from dimer formation needs to be taken into account in all the environments
436   especially those with higher cluster formation probabilities due to availability of stabilizing bases.

437

438   The coefficients derived do not differ substantially between the different locations. The proxy could
439   therefore be used at locations with no prior H_2SO_4 measurements, provided that the environmental
440   conditions are approximately similar to those in one of the four sites described here. More specifically,
441   the proxies could be utilized to derive long-term data sets for H_2SO_4 concentrations, which would be
442   essential in performing various kinds of trend analyses. In order to derive the long term sulphuric acid
443   concentrations, we recommend deriving in-house coefficients in case sulphuric acid concentrations
444   are directly measured rather than using the ones from already derived studies. The choice of equation
445   depends on the availability of the data on site. In case alkenes or their proxies are measured and
446   sulphuric acid is measured, derivation of the coefficients should be based on Equation 2. In case
447   neither alkenes nor their proxies are measured but sulphuric acid is measured, the coefficients and
448   therefore the proxy for daytime only can be derived, using Equation 4. In case, sulphuric acid is not
449   measured, one can calculate the sulphuric acid proxy using the Equation 2 or Equation 4, depending
450   on whether the alkene data is available or not, respectively, using the coefficients suggested in Table

451 1 which are relevant to the site of interest. In order to make the best choice for the coefficients, Figure
452 10 can be followed in order to decide which description fits the location of interest best. For instance,
453 in case the condensation sink is between 2×10^{-3} and 6×10^{-3} s^{-1}, and the SO_2 concentration is lower
454 than 2×10^9 molecules. cm^{-3}, coefficients of Hyytiälä or the boreal forest are to be used.
455

Data availability
457 The data used in the manuscript and the MATLAB code which provides the k values are available
458 from the first author at lubna.dada@helsinki.fi.
459

Author contributions
461 MK came up with the idea, LD, IY, CL, RB analyzed the data, YG, CD, RY, CY, LY, JJ, YL, BC
462 performed the measurements in Beijing and pre-processed the raw data, NS, TJ, MS, TP performed
463 the measurements in Hyytiälä and pre-processed the raw data, LD, TN, JK, KRD, DS, TH, PP, FB,
464 VMK, MK provided useful discussion and ideas, IS, TW, RB, TJ performed the measurements in
465 Budapest and pre-processed the raw data, MP, JS, RB, TJ performed the measurement in Agia Marina
466 and pre-processed the raw data. LD, VMK and MK wrote the manuscript. All co-authors contributed
467 to reviewing the manuscript and to the discussions related to it.
468

Competing interests
470 All authors declare no competing interests.
471

472

Acknowledgements
474

475 This project has received funding from the ERC advanced grant No. 742206, ERC-StG No. 714621,
476 the Academy of Finland Center of Excellence project No. 307331, Academy of Finland project No.
477 316114 and 296628, the National Natural Science Foundation of China project No. 41877306 and
478 from National Key R&D Program of China (2017YFC0209503). This project receives funding from
479 the European Union's Horizon 2020 research and innovation program under grant agreements
480 (ACTRIS) No. 654109 and 739530. Funding by the National Research, Development and Innovation
481 Office, Hungary (K116788 and K132254) is acknowledged. We thank V. Varga and Z. Németh of the
482 Eötvös University for their help in the experimental work in Budapest and K. Neitola and T. Laurila
483 for their help at Agia Marina. This publication has been produced within the framework of the
484 EMME-CARE project which has received funding from the European Union's Horizon 2020
485 Research and Innovation Programme, under Grant Agreement No. 856612 and the Cyprus
486 Government. The sole responsibility of this publication lies with the author. The European Union is
487 not responsible for any use that may be made of the information contained therein.
488

489

490   **Tables and Figures**

491

492   Table 1: Coefficients used in the proxy equation in all four environments. Numbers in parenthesis

493   represent the 25th and 75th percentiles of boot strapped data, respectively.

494

Location	*GlobRad (W/m²)*	$k_1(10^{-8}$ m² W⁻¹ s⁻¹)	$k_2(\cdot10^{-29}$ cm⁶ s⁻¹)	k_3 ($\cdot10^{-9}$ cm³ s⁻¹)
Hyytiälä	>=0	1.21(1.15-1.24)	10.3(10.0-10.61)	5.98(5.58-5.99)
Agia Marina	>= 50	0.92(0.78-1.13)	N/A	2.32(1.47-3.63)
Budapest	>= 50	0.14(0.13-0.15)	N/A	7.90(7.90-7.91)
Beijing	>= 50	5.20(4.62 – 5.78)	1.45(1.09 – 1.88)	5.76(4.30 – 7.0)
Beijing	<50	1.35(1.09 – 1.64)	4.39(4.24 – 4.59)	7.0(6.99 – 7.0)

495

496   Table 2: Fraction of each source and sink term to total H_2SO_4 concentration. Median of boot strapping

497   results and their 25th and 27th percentiles are shown.

498

	GlobRad (W/m²)	Source Terms		Sink Terms	
		$k_1 Glob[SO_2]$	$k_2[O_3][A][SO_2]$	$-k_3[H_2SO_4]^2$	$-CS[H_2SO_4]$
Hyytiälä	>=0	0.31 (0.08-0.43)	0.18 (0.06-0.41)	0.16 (0.06-0.29)	0.34 (0.21-0.44)
Agia Marina	>= 50	0.5 (0.48-0.52)	0	0.20 (0.15-0.32)	0.30 (0.18-0.33)
Budapest	>= 50	0.5 (0.48-0.51)	0	0.22 (0.15-0.29)	0.28 (0.21-0.35)
Beijing	>= 50	0.29 (0.24 – 0.35)	0.21 (0.15 – 0.26)	0.29 (0.18 – 0.34)	0.21 (0.14 – 0.30)
	<50	0.06 (0.02 – 0.13)	0.44 (0.36 – 0.48)	0.24 (0.11-0.35)	0.26 (0.15-0.39)

499

500

501

502
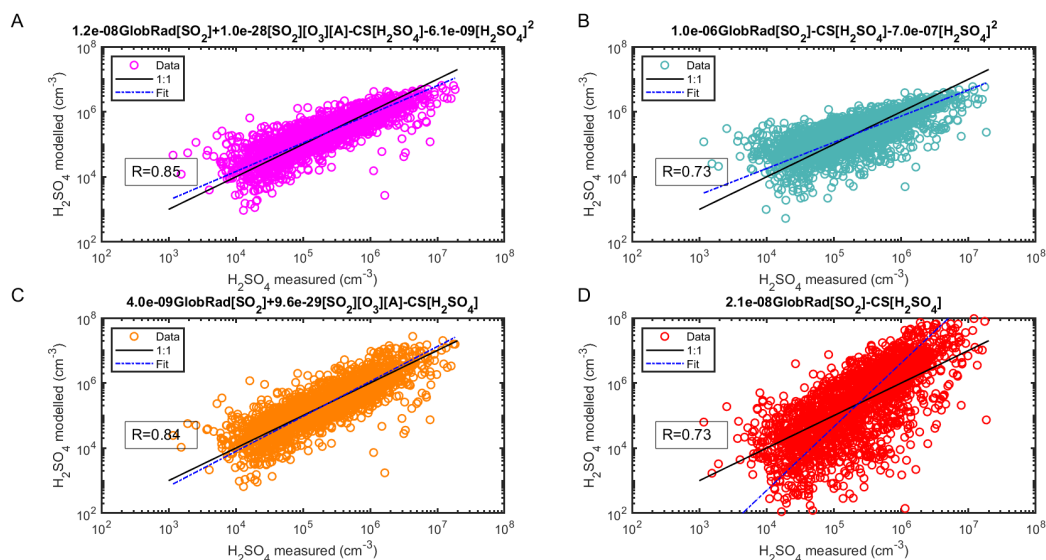
Figure 1: Sulphuric acid proxy concentration as a function of measured sulphuric acid. Observation at SMEAR II station, Hyytiälä Finland. The observed concentrations are measured 2016-2019 using CI-APi-ToF and are 1-hour medians resulting in a total of 2089 data points. In (A), the full Equation 2 is used, in (B) the equation without the Stabilized Criegee Intermediates source (Equation 4), in (C) the equation without the cluster sink term (Equation 5) and in (D) the equation without both the Stabilized Criegee Intermediates source and the cluster sink term (Equation 6). The 'Fit' refers to the fitting between the measured and the proxy calculated sulphuric acid concentration.

510

511
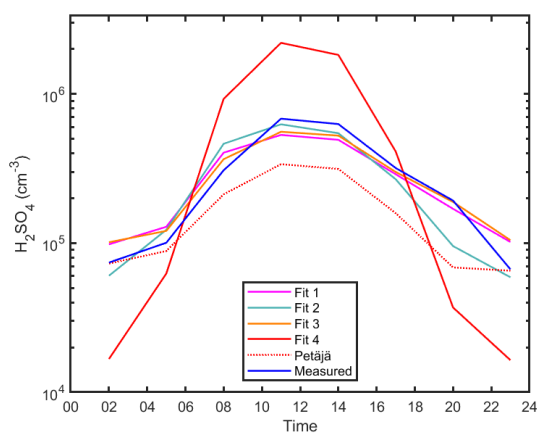
Figure 2: The diurnal variation of sulphuric acid proxy concentrations using different fits and observed concentrations at SMEAR II in Hyytiälä, Finland. Median values are shown. Fits 1,2, 3 and 4 corresponds to the Equations 2, 4, 5, and 6, respectively. Petäjä fit shown is applied using the coefficients reported in Petäjä et al. 2009 (Equation 7).

516

517
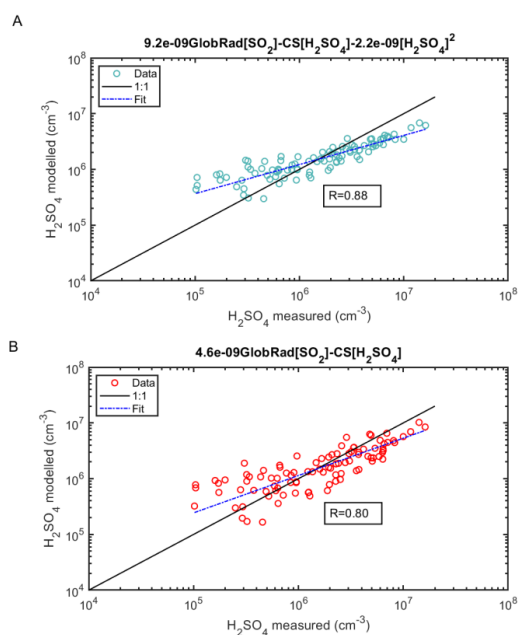
518
519 *Figure 3: Sulphuric acid proxy concentration as a function of measured sulphuric acid. Observation*
520 *at Agia Marina, Cyprus, excluding the Alkene term. The observed numbers concentrations are*
521 *measured during Feb- Mar 2018 using CI-APi-ToF and are hourly medians resulting in a total of 96*
522 *data points. Sulphuric acid proxy concentration as a function of measured sulphuric acid. In (A), the*
523 *equation without the Stabilized Criegee Intermediates source (Equation 4) and in (B) the equation*
524 *without both the Stabilized Criegee Intermediates source and the cluster sink term (Equation 6).*
525
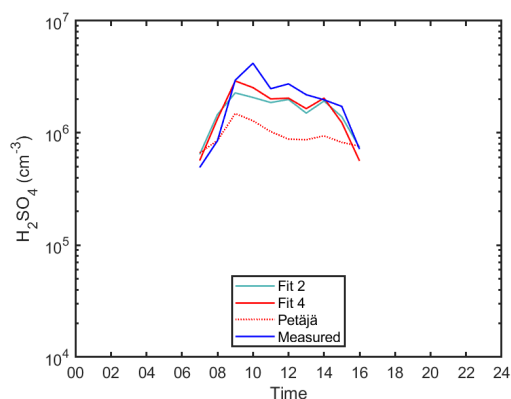
526
527 *Figure 4 The diurnal variation of sulphuric acid proxies and observed concentrations in Agia Marina,*
528 *Cyprus. Hourly median values are shown. Fits 2 and 4 corresponds to the Equations 4 and 6,*
529 *respectively, See also Figure 3A and B, respectively. Petäjä fit shown is applied using the coefficients*
530 *reported in Petäjä et al. 2009 (Equation 7).*
531
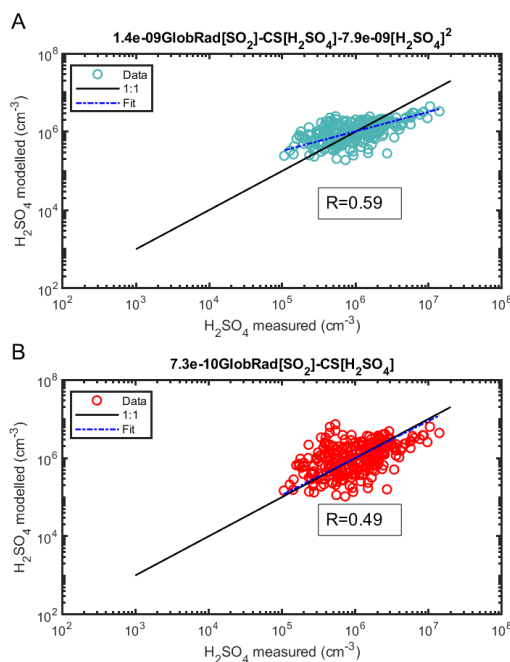
532
533
534 *Figure 5 Sulphuric acid proxy as a function measured sulphuric acid at Budapest station, excluding*
535 *the Alkene term. The observed numbers are measured during spring 2018 using CI-APi-ToF and are*
536 *1-hour medians coinciding with the measurement of trace gases and Global radiation every one hour*
537 *resulting in a total of 262 data points. In (A), the equation without the Stabilized Criegee*
538 *Intermediates source (Equation 4) and in (B) the equation without both the Stabilized Criegee*
539 *Intermediates source and the cluster sink term (Equation 6).*
540
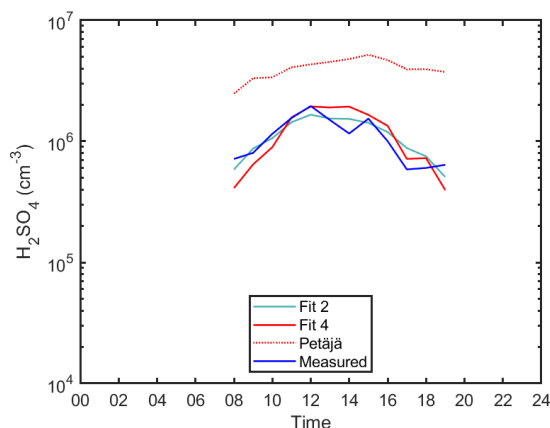
541
542 *Figure 6 The diurnal variation of sulphuric acid proxies and measured concentrations in Budapest.*
543 *Hourly median values are shown. Fits 2 and 4 corresponds to the Equations 4 and 6, respectively.*
544 *Petäjä fit shown is applied using the coefficients reported in Petäjä et al. 2009 (Equation 7).*
545

546
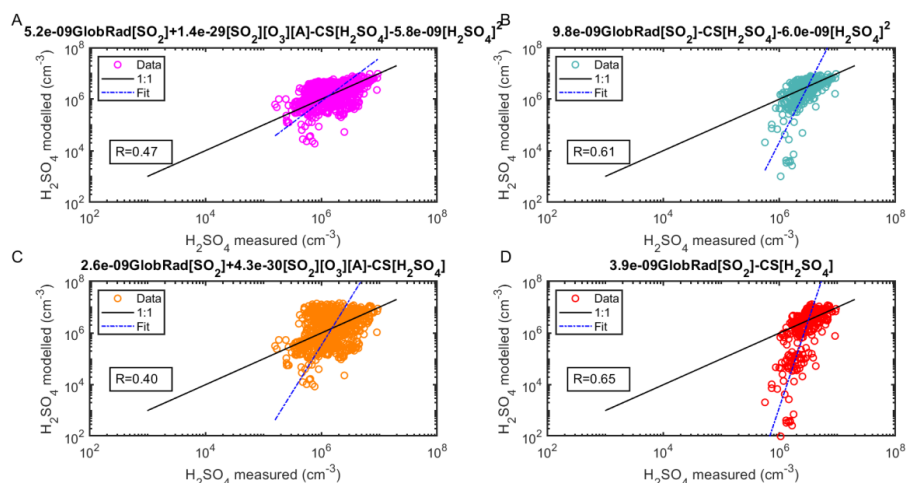
Figure 7 (A) Sulphuric acid proxy concentration using Globrad as a function of measured sulphuric
acid. Observation at Beijing, China. The observed numbers concentrations are measured between
2018-2019 using CI-APi-ToF and are 1-hour medians resulting in a total of 875 data points. In (A),
the full Equation 2 is used, in (B) the equation without the Stabilized Criegee Intermediates source
(Equation 4), in (C) the equation without the cluster sink term (Equation 5) and in (D) the equation
without both the Stabilized Criegee Intermediates source and the cluster sink term (Equation 6).
Coefficients shown on top of the subplots relate to the daytime values.

554
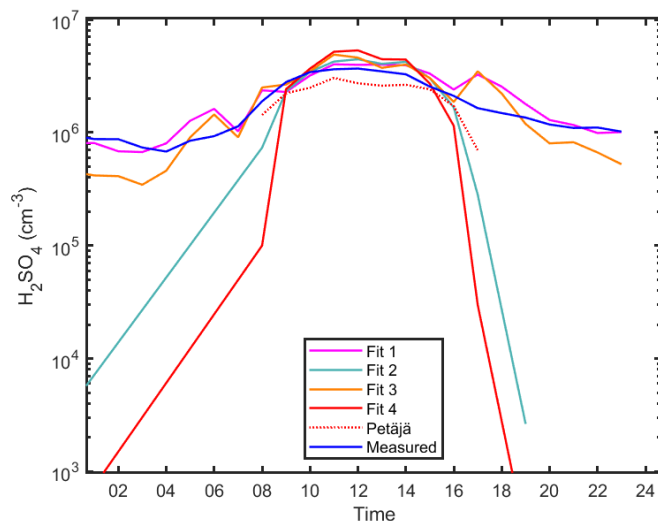
Figure 8 The diurnal variation of sulphuric acid proxy concentrations using different fits and
observed concentrations at Beijing China, Finland. Median values are shown. Fits 1,2, 3 and 4
corresponds to the Equations 2, 4, 5, and 6, respectively. Petäjä fit shown is applied using the
coefficients reported in Petäjä et al. 2009 (Equation 7).

559
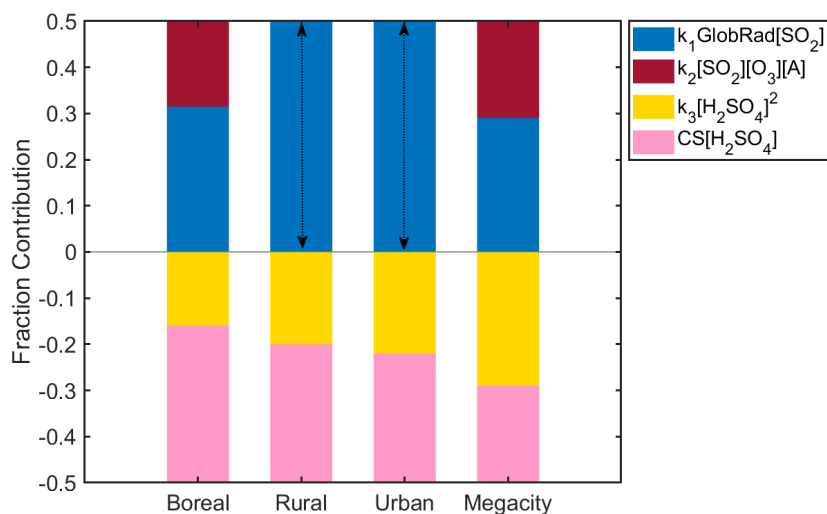
560

561 *Figure 9 Fraction of each source and sink term to the change in H_2SO_4 concentration during daytime.*
562 *Figure 9 is complementary to Table 2. The boreal, rural, urban and megacity labels refer to Hyytiälä,*
563 *Agia Marina, Budapest and Beijing sites, respectively. Note that the fraction of the alkene term*
564 *contribution is not zero for the rural or urban sites, but is due to unavailable alkene data from the*
565 *Budapest and Cyprus sites.*

566
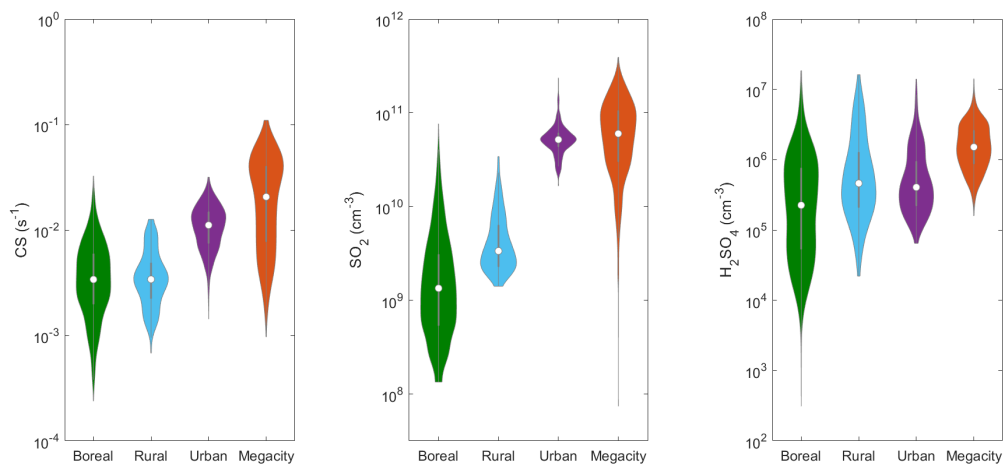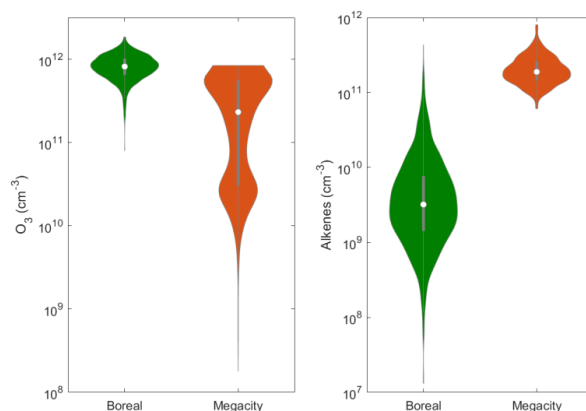
Figure 10 Condensation Sink, SO_2 and H_2SO_4 concentrations in diffrerent environements and O_3 and Alkenes in the boreal forest (Hyytiälä) and megacity (Beijing) environments. This figure could be used in order to choose the coefficients for calculating the proxy. The alkenes in the boreal environment are monoterpenes(e.g. alpha-pinene) and in the Megacity are anthropogenic volatile organic compounds (propylene, butylene, butadiene, isoprene, pentene and hexene). The concentrations are displayed as violin plots which are a combination of boxplot and a kernel distribution function on each side of the boxplots. The white circles define the median of the distribution and the edges on the inner grey boxes refer to the 25th and 75th percentiles respectively. Daytime data (GlobRad > 50 W/m^2) is shown in Figure S11-S12. The correlations between the different variables at each site are shown in Figures S3 – S7.

578 **References**

579

580 Aalto, P., Hameri, K., Becker, E., Weber, R., Salm, J., Makela, J. M., Hoell, C., O'Dowd, C. D.,
581   Karlsson, H., Hansson, H. C., Vakeva, M., Koponen, I. K., Buzorius, G., and Kulmala, M.:
582   Physical characterization of aerosol particles during nucleation events, Tellus B, 53, 344-
583   358, DOI 10.1034/j.1600-0889.2001.530403.x, 2001.

584

585 Almeida, J., Schobesberger, S., Kurten, A., Ortega, I. K., Kupiainen-Maatta, O., Praplan, A. P.,
586   Adamov, A., Amorim, A., Bianchi, F., Breitenlechner, M., David, A., Dommen, J., Donahue,
587   N. M., Downard, A., Dunne, E., Duplissy, J., Ehrhart, S., Flagan, R. C., Franchin, A., Guida,
588   R., Hakala, J., Hansel, A., Heinritzi, M., Henschel, H., Jokinen, T., Junninen, H., Kajos, M.,
589   Kangasluoma, J., Keskinen, H., Kupc, A., Kurten, T., Kvashin, A. N., Laaksonen, A.,
590   Lehtipalo, K., Leiminger, M., Leppa, J., Loukonen, V., Makhmutov, V., Mathot, S.,
591   McGrath, M. J., Nieminen, T., Olenius, T., Onnela, A., Petaja, T., Riccobono, F., Riipinen, I.,
592   Rissanen, M., Rondo, L., Ruuskanen, T., Santos, F. D., Sarnela, N., Schallhart, S.,
593   Schnitzhofer, R., Seinfeld, J. H., Simon, M., Sipila, M., Stozhkov, Y., Stratmann, F., Tome,
594   A., Trostl, J., Tsagkogeorgas, G., Vaattovaara, P., Viisanen, Y., Virtanen, A., Vrtala, A.,
595   Wagner, P. E., Weingartner, E., Wex, H., Williamson, C., Wimmer, D., Ye, P. L., Yli-Juuti, T.,
596   Carslaw, K. S., Kulmala, M., Curtius, J., Baltensperger, U., Worsnop, D. R., Vehkamaki, H.,
597   and Kirkby, J.: Molecular understanding of sulphuric acid-amine particle nucleation in the
598   atmosphere, Nature, 502, 359-363, 10.1038/nature12663, 2013.

599

600 Berresheim, H., Elste, T., Tremmel, H. G., Allen, A. G., Hansson, H. C., Rosman, K., Dal Maso, M.,
601   Makela, J. M., Kulmala, M., and O'Dowd, C. D.: Gas-aerosol relationships of H2SO4,
602   MSA, and OH: Observations in the coastal marine boundary layer at Mace Head, Ireland, J
603   Geophys Res-Atmos, 107, Artn 8100
604 10.1029/2000jd000229, 2002.

605

606 Chu, B., Kerminen, V. M., Bianchi, F., Yan, C., Petäjä, T., and Kulmala, M.: Atmospheric new
607   particle formation in China, Atmos. Chem. Phys., 19, 115-138, 10.5194/acp-19-115-2019,
608   2019.

609

610 Efron, B., and Tibshirani, R. J.: An introduction to the bootstrap, CRC press, 1994.

611

612 Eisele, F. L., and Tanner, D. J.: Measurement of the Gas-Phase Concentration of H2so4 and
613   Methane Sulfonic-Acid and Estimates of H2so4 Production and Loss in the Atmosphere, J
614   Geophys Res-Atmos, 98, 9001-9010, Doi 10.1029/93jd00031, 1993.

615

616 Erupe, M. E., Viggiano, A. A., and Lee, S. H.: The effect of trimethylamine on atmospheric
617   nucleation involving H2SO4, Atmos. Chem. Phys., 11, 4767-4775, 10.5194/acp-11-4767-
618   2011, 2011.

619

620 Gao, W., Tan, G., Hong, Y., Li, M., Nian, H., Guo, C., Huang, Z., Fu, Z., Dong, J., Xu, X., Cheng,
621   P., and Zhou, Z.: Development of portable single photon ionization time-of-flight mass
622   spectrometer combined with membrane inlet, International Journal of Mass Spectrometry,
623   334, 8-12, https://doi.org/10.1016/j.ijms.2012.09.003, 2013.

624

625 Gordon, H., Kirkby, J., Baltensperger, U., Bianchi, F., Breitenlechner, M., Curtius, J., Dias, A.,
626   Dommen, J., Donahue, N. M., Dunne, E. M., Duplissy, J., Ehrhart, S., Flagan, R. C., Frege,
627   C., Fuchs, C., Hansel, A., Hoyle, C. R., Kulmala, M., Kurten, A., Lehtipalo, K., Makhmutov,
628   V., Molteni, U., Rissanen, M. P., Stozhkov, Y., Trostl, J., Tsagkogeorgas, G., Wagner, R.,
629   Williamson, C., Wimmer, D., Winkler, P. M., Yan, C., and Carslaw, K. S.: Causes and

630   importance of new particle formation in the present-day and preindustrial atmospheres, J
631   Geophys Res-Atmos, 122, 8739-8760, 10.1002/2017jd026844, 2017.
632
633   Guo, S., Hu, M., Zamora, M. L., Peng, J., Shang, D., Zheng, J., Du, Z., Wu, Z., Shao, M., Zeng, L.,
634   Molina, M. J., and Zhang, R.: Elucidating severe urban haze formation in China,
635   Proceedings of the National Academy of Sciences, 111, 17373-17378,
636   10.1073/pnas.1419604111 2014.
637
638   Hakola, H., Hellen, H., Hemmila, M., Rinne, J., and Kulmala, M.: In situ measurements of volatile
639   organic compounds in a boreal forest, Atmos Chem Phys, 12, 11665-11678, 10.5194/acp-12-
640   11665-2012, 2012.
641
642   Hari, P., and Kulmala, M.: Station for measuring ecosystem-atmosphere relations (SMEAR II),
643   Boreal Environ Res, 10, 315-322, 2005.
644
645   Hellén, H., Praplan, A. P., Tykkä, T., Ylivinkka, I., Vakkari, V., Bäck, J., Petäjä, T., Kulmala, M.,
646   Hakola, H. J. A. C., and Physics: Long-term measurements of volatile organic compounds
647   highlight the importance of sesquiterpenes for the atmospheric chemistry of a boreal forest,
648   18, 13839-13863, 2018.
649
650   Jen, C. N., McMurry, P. H., and Hanson, D. R.: Stabilization of sulphuric acid dimers by ammonia,
651   methylamine, dimethylamine, and trimethylamine, Journal of Geophysical Research:
652   Atmospheres, 119, 7502-7514, 2014.
653
654   Jokinen, T., Sipila, M., Junninen, H., Ehn, M., Lonn, G., Hakala, J., Petaja, T., Mauldin, R. L.,
655   Kulmala, M., and Worsnop, D. R.: Atmospheric sulphuric acid and neutral cluster
656   measurements using CI-APi-TOF, Atmos Chem Phys, 12, 4117-4125, 10.5194/acp-12-4117-
657   2012, 2012.
658
659   Junninen, H., Ehn, M., Petaja, T., Luosujarvi, L., Kotiaho, T., Kostiainen, R., Rohner, U., Gonin,
660   M., Fuhrer, K., Kulmala, M., and Worsnop, D. R.: A high-resolution mass spectrometer to
661   measure atmospheric ion composition, Atmos Meas Tech, 3, 1039-1053, 10.5194/amt-3-
662   1039-2010, 2010.
663
664   Kerminen, V.-M., Paramonov, M., Anttila, T., Riipinen, I., Fountoukis, C., Korhonen, H., Asmi, E.,
665   Laakso, L., Lihavainen, H., Swietlicki, E., Svenningsson, B., Asmi, A., Pandis, S. N.,
666   Kulmala, M., and Petäjä, T.: Cloud condensation nuclei production associated with
667   atmospheric nucleation: a synthesis based on existing literature and new results, Atmos.
668   Chem. Phys., 12, 12037-12059, 10.5194/acp-12-12037-2012, 2012.
669
670   Kerminen, V.-M., Chen, X., Vakkari, V., Petäjä, T., Kulmala, M., and Bianchi, F.: Atmospheric new
671   particle formation and growth: review of field observations, Environ. Res. Lett., 13, 103003,
672   10.1088/1748-9326/aadf3c, 2018.
673
674   Kulmala, M., Vehkamäki, H., Petäjä, T., Dal Maso, M., Lauri, A., Kerminen, V.-M., Birmili, W., and
675   McMurry, P. H.: Formation and growth rates of ultrafine atmospheric particles: a review of
676   observations, J Aerosol Sci, 35, 143-176, 10.1016/j.jaerosci.2003.10.003, 2004.
677
678   Kulmala, M., Petaja, T., Nieminen, T., Sipila, M., Manninen, H. E., Lehtipalo, K., Dal Maso, M.,
679   Aalto, P. P., Junninen, H., Paasonen, P., Riipinen, I., Lehtinen, K. E. J., Laaksonen, A., and
680   Kerminen, V. M.: Measurement of the nucleation of atmospheric aerosol particles, Nat
681   Protoc, 7, 1651-1667, 10.1038/nprot.2012.091, 2012.

682

683 Kulmala, M., Kontkanen, J., Junninen, H., Lehtipalo, K., Manninen, H. E., Nieminen, T., Petaja, T.,
684   Sipila, M., Schobesberger, S., Rantala, P., Franchin, A., Jokinen, T., Jarvinen, E., Aijala, M.,
685   Kangasluoma, J., Hakala, J., Aalto, P. P., Paasonen, P., Mikkila, J., Vanhanen, J., Aalto, J.,
686   Hakola, H., Makkonen, U., Ruuskanen, T., Mauldin, R. L., Duplissy, J., Vehkamaki, H.,
687   Back, J., Kortelainen, A., Riipinen, I., Kurten, T., Johnston, M. V., Smith, J. N., Ehn, M.,
688   Mentel, T. F., Lehtinen, K. E. J., Laaksonen, A., Kerminen, V. M., and Worsnop, D. R.:
689   Direct Observations of Atmospheric Aerosol Nucleation, Science, 339, 943-946,
690   10.1126/science.1227385, 2013.
691

692 Kulmala, M., Kerminen, V. M., Petaja, T., Ding, A. J., and Wang, L.: Atmospheric gas-to-particle
693   conversion: why NPF events are observed in megacities?, Faraday Discuss, 200, 271-288,
694   10.1039/c6fd00257a, 2017.
695

696 Kürten, A., Williamson, C., Almeida, J., Kirkby, J., and Curtius, J.: On the derivation of particle
697   nucleation rates from experimental formation rates, Atmos. Chem. Phys., 15, 4063-4075,
698   10.5194/acp-15-4063-2015, 2015.
699

700 Laakso, L., Petaja, T., Lehtinen, K. E. J., Kulmala, M., Paatero, J., Horrak, U., Tammet, H., and
701   Joutsensaari, J.: Ion production rate in a boreal forest based on ion, particle and radiation
702   measurements, Atmos Chem Phys, 4, 1933-1943, DOI 10.5194/acp-4-1933-2004, 2004.
703

704 Laakso, L., Koponen, I. K., Monkkonen, P., Kulmala, M., Kerminen, V. M., Wehner, B.,
705   Wiedensohler, A., Wu, Z. J., and Hu, M.: Aerosol particles in the developing world; A
706   comparison between New Delhi in India and Beijing in China, Water Air Soil Poll, 173, 5-
707   20, 10.1007/s11270-005-9018-5, 2006.
708

709 Lagarias, J. C., Reeds, J. A., Wright, M. H., and Wright, P. E.: Convergence Properties of the
710   Nelder--Mead Simplex Method in Low Dimensions, SIAM Journal on Optimization, 9, 112-
711   147, 10.1137/s1052623496303470, 1998.
712

713 Lehtipalo, K., Yan, C., Dada, L., Bianchi, F., Xiao, M., Wagner, R., Stolzenburg, D., Ahonen, L. R.,
714   Amorim, A., Baccarini, A., Bauer, P. S., Baumgartner, B., Bergen, A., Bernhammer, A.-K.,
715   Breitenlechner, M., Brilke, S., Buchholz, A., Mazon, S. B., Chen, D., Chen, X., Dias, A.,
716   Dommen, J., Draper, D. C., Duplissy, J., Ehn, M., Finkenzeller, H., Fischer, L., Frege, C.,
717   Fuchs, C., Garmash, O., Gordon, H., Hakala, J., He, X., Heikkinen, L., Heinritzi, M., Helm,
718   J. C., Hofbauer, V., Hoyle, C. R., Jokinen, T., Kangasluoma, J., Kerminen, V.-M., Kim, C.,
719   Kirkby, J., Kontkanen, J., Kürten, A., Lawler, M. J., Mai, H., Mathot, S., Mauldin, R. L.,
720   Molteni, U., Nichman, L., Nie, W., Nieminen, T., Ojdanic, A., Onnela, A., Passananti, M.,
721   Petäjä, T., Piel, F., Pospisilova, V., Quéléver, L. L. J., Rissanen, M. P., Rose, C., Sarnela, N.,
722   Schallhart, S., Schuchmann, S., Sengupta, K., Simon, M., Sipilä, M., Tauber, C., Tomé, A.,
723   Tröstl, J., Väisänen, O., Vogel, A. L., Volkamer, R., Wagner, A. C., Wang, M., Weitz, L.,
724   Wimmer, D., Ye, P., Ylisirniö, A., Zha, Q., Carslaw, K. S., Curtius, J., Donahue, N. M.,
725   Flagan, R. C., Hansel, A., Riipinen, I., Virtanen, A., Winkler, P. M., Baltensperger, U.,
726   Kulmala, M., and Worsnop, D. R.: Multicomponent new particle formation from sulphuric
727   acid, ammonia, and biogenic vapors, Science Advances, 4, eaau5363,
728   10.1126/sciadv.aau5363 2018.
729

730 Liu, J., Jiang, J., Zhang, Q., Deng, J., Hao, J. J. F. o. E. S., and Engineering: A spectrometer for
731   measuring particle size distributions in the range of 3 nm to 10 μm, 10, 63-72,
732   10.1007/s11783-014-0754-x, 2016.
733

734 Lu, Y., Yan, C., Fu, Y., Chen, Y., Liu, Y., Yang, G., Wang, Y., Bianchi, F., Chu, B., Zhou, Y., Yin, R.,
735   Baalbaki, R., Garmash, O., Deng, C., Wang, W., Liu, Y., Petäjä, T., Kerminen, V. M., Jiang,
736   J., Kulmala, M., and Wang, L.: A proxy for atmospheric daytime gaseous sulphuric acid
737   concentration in urban Beijing, Atmos. Chem. Phys., 19, 1971-1983, 10.5194/acp-19-1971-
738   2019, 2019.
739
740 Ma, F., Xie, H.-B., Elm, J., Shen, J., Chen, J., and Vehkamäki, H.: Piperazine Enhancing Sulphuric
741   Acid-Based New Particle Formation: Implications for the Atmospheric Fate of Piperazine,
742   Environ Sci Technol, 53, 8785-8795, 10.1021/acs.est.9b02117, 2019.
743
744 Mauldin, R. L., Berndt, T., Sipila, M., Paasonen, P., Petaja, T., Kim, S., Kurten, T., Stratmann, F.,
745   Kerminen, V. M., and Kulmala, M.: A new atmospherically relevant oxidant of sulphur
746   dioxide, Nature, 488, 193-196, 10.1038/nature11278, 2012.
747
748 McElreath, R.: Statistical rethinking: A Bayesian course with examples in R and Stan, Chapman and
749   Hall/CRC, 2018.
750
751 Merikanto, J., Spracklen, D. V., Mann, G. W., Pickering, S. J., and Carslaw, K. S.: Impact of
752   nucleation on global CCN, Atmos Chem Phys, 9, 8601-8616, 10.5194/acp-9-8601-2009,
753   2009.
754
755 Mikkonen, S., Romakkaniemi, S., Smith, J. N., Korhonen, H., Petaja, T., Plass-Duelmer, C., Boy,
756   M., McMurry, P. H., Lehtinen, K. E. J., Joutsensaari, J., Hamed, A., Mauldin, R. L., Birmili,
757   W., Spindler, G., Arnold, F., Kulmala, M., and Laaksonen, A.: A statistical proxy for
758   sulphuric acid concentration, Atmos Chem Phys, 11, 11319-11334, 10.5194/acp-11-11319-
759   2011, 2011.
760
761 Monkkonen, P., Koponen, I. K., Lehtinen, K. E. J., Uma, R., Srinivasan, D., Hameri, K., and
762   Kulmala, M.: Death of nucleation and Aitken mode particles: observations at extreme
763   atmospheric conditions and their theoretical explanation, J Aerosol Sci, 35, 781-787,
764   10.1016/j.jaerosci.2003.12.004, 2004.
765
766 Monkkonen, P., Koponen, I. K., Lehtinen, K. E. J., Hameri, K., Uma, R., and Kulmala, M.:
767   Measurements in a highly polluted Asian mega city: observations of aerosol number size
768   distribution, modal parameters and nucleation events, Atmos Chem Phys, 5, 57-66, 2005.
769
770 Nieminen, T., Kerminen, V. M., Petäjä, T., Aalto, P. P., Arshinov, M., Asmi, E., Baltensperger, U.,
771   Beddows, D. C. S., Beukes, J. P., Collins, D., Ding, A., Harrison, R. M., Henzing, B.,
772   Hooda, R., Hu, M., Hõrrak, U., Kivekäs, N., Komsaare, K., Krejci, R., Kristensson, A.,
773   Laakso, L., Laaksonen, A., Leaitch, W. R., Lihavainen, H., Mihalopoulos, N., Németh, Z.,
774   Nie, W., O'Dowd, C., Salma, I., Sellegri, K., Svenningsson, B., Swietlicki, E., Tunved, P.,
775   Ulevicius, V., Vakkari, V., Vana, M., Wiedensohler, A., Wu, Z., Virtanen, A., and Kulmala,
776   M.: Global analysis of continental boundary layer new particle formation based on long-
777   term measurements, Atmos. Chem. Phys., 18, 14737-14756, 10.5194/acp-18-14737-2018,
778   2018.
779
780 Novelli, A., Hens, K., Ernest, C. T., Martinez, M., Nolscher, A. C., Sinha, V., Paasonen, P., Petaja,
781   T., Sipila, M., Elste, T., Plass-Dulmer, C., Phillips, G. J., Kubistin, D., Williams, J.,
782   Vereecken, L., Lelieveld, J., and Harder, H.: Estimating the atmospheric concentration of
783   Criegee intermediates and their possible interference in a FAGE-LIF instrument, Atmos
784   Chem Phys, 17, 7807-7826, 10.5194/acp-17-7807-2017, 2017.
785

786 Petäjä, T., Mauldin, R. L., Kosciuch, E., McGrath, J., Nieminen, T., Paasonen, P., Boy, M., Adamov,
787   A., Kotiaho, T., and Kulmala, M.: Sulphuric acid and OH concentrations in a boreal forest
788   site, Atmos Chem Phys, 9, 7435-7448, DOI 10.5194/acp-9-7435-2009, 2009.
789
790 Pikridas, M., Vrekoussis, M., Sciare, J., Kleanthous, S., Vasiliadou, E., Kizas, C., Savvides, C., and
791   Mihalopoulos, N.: Spatial and temporal (short and long-term) variability of submicron, fine
792   and sub-10 μm particulate matter (PM1, PM2.5, PM10) in Cyprus, Atmos Environ, 191, 79-
793   93, https://doi.org/10.1016/j.atmosenv.2018.07.048, 2018.
794
795 Rinne, J., Ruuskanen, T. M., Reissell, A., Taipale, R., Hakola, H., and Kulmala, M.: On-line PTR-
796   MS measurements of atmospheric concentrations of volatile organic compounds in a
797   European boreal forest ecosystem, Boreal Environ Res, 10, 425-436, 2005.
798
799 Rohrer, F., and Berresheim, H.: Strong correlation between levels of tropospheric hydroxyl radicals
800   and solar ultraviolet radiation, Nature, 442, 184-187, 10.1038/nature04924, 2006.
801
802 Salma, I., Németh, Z., Kerminen, V.-M., Aalto, P., Nieminen, T., Weidinger, T., Molnár, Á., Imre,
803   K., and Kulmala, M.: Regional effect on urban atmospheric nucleation, Atmos Chem Phys,
804   16, 8715-8728, 2016.
805
806 Salma, I., and Németh, Z.: Dynamic and timing properties of new aerosol particle formation and
807   consecutive growth events, Atmos. Chem. Phys., 19, 5835-5852, 10.5194/acp-19-5835-
808   2019, 2019.
809
810 Sihto, S. L., Kulmala, M., Kerminen, V. M., Dal Maso, M., Petaja, T., Riipinen, I., Korhonen, H.,
811   Arnold, F., Janson, R., Boy, M., Laaksonen, A., and Lehtinen, K. E. J.: Atmospheric
812   sulphuric acid and aerosol formation: implications from atmospheric measurements for
813   nucleation and early growth mechanisms, Atmos Chem Phys, 6, 4079-4091, DOI
814   10.5194/acp-6-4079-2006, 2006.
815
816 Sipilä, M., Berndt, T., Petäjä, T., Brus, D., Vanhanen, J., Stratmann, F., Patokoski, J., Mauldin, R.
817   L., Hyvärinen, A.-P., Lihavainen, H., and Kulmala, M.: The Role of Sulphuric Acid in
818   Atmospheric Nucleation, Science, 327, 1243-1246, 10.1126/science.1180315 2010.
819
820 Sipilä, M., Jokinen, T., Berndt, T., Richters, S., Makkonen, R., Donahue, N. M., Mauldin, R. L.,
821   Kurten, T., Paasonen, P., Sarnela, N., Ehn, M., Junninen, H., Rissanen, M. P., Thornton, J.,
822   Stratmann, F., Herrmann, H., Worsnop, D. R., Kulmala, M., Kerminen, V. M., and Petäjä, T.:
823   Reactivity of stabilized Criegee intermediates (sCIs) from isoprene and monoterpene
824   ozonolysis toward SO2 and organic acids, Atmos Chem Phys, 14, 12143-12153,
825   10.5194/acp-14-12143-2014, 2014.
826
827 Spracklen, D. V., Carslaw, K. S., Kulmala, M., Kerminen, V. M., Sihto, S. L., Riipinen, I.,
828   Merikanto, J., Mann, G. W., Chipperfield, M. P., and Wiedensohler, A.: Contribution of
829   particle formation to global cloud condensation nuclei concentrations, Geophy. Res. Lett.,
830   35, 2008.
831
832 Spracklen, D. V., Carslaw, K. S., Merikanto, J., Mann, G. W., Reddington, C. L., Pickering, S.,
833   Ogren, J. A., Andrews, E., Baltensperger, U., Weingartner, E., Boy, M., Kulmala, M.,
834   Laakso, L., Lihavainen, H., Kivekas, N., Komppula, M., Mihalopoulos, N., Kouvarakis, G.,
835   Jennings, S. G., O'Dowd, C., Birmili, W., Wiedensohler, A., Weller, R., Gras, J., Laj, P.,
836   Sellegri, K., Bonn, B., Krejci, R., Laaksonen, A., Hamed, A., Minikin, A., Harrison, R. M.,
837   Talbot, R., and Sun, J.: Explaining global surface aerosol number concentrations in terms of

838   primary emissions and particle formation, Atmos Chem Phys, 10, 4775-4793, 10.5194/acp-
839   10-4775-2010, 2010.
840
841 Taipale, R., Ruuskanen, T. M., Rinne, J., Kajos, M. K., Hakola, H., Pohja, T., and Kulmala, M.:
842   Technical Note: Quantitative long-term measurements of VOC concentrations by PTR-MS -
843   measurement, calibration, and volume mixing ratio calculation methods, Atmos Chem Phys,
844   8, 6681-6698, DOI 10.5194/acp-8-6681-2008, 2008.
845
846 Weber, R. J., Marti, J. J., McMurry, P. H., Eisele, F. L., Tanner, D. J., and Jefferson, A.:
847   MEASURED ATMOSPHERIC NEW PARTICLE FORMATION RATES: IMPLICATIONS
848   FOR NUCLEATION MECHANISMS, Chemical Engineering Communications, 151, 53-64,
849   10.1080/00986449608936541, 1996.
850
851 Yan, C., Dada, L., Rose, C., Jokinen, T., Nie, W., Schobesberger, S., Junninen, H., Lehtipalo, K.,
852   Sarnela, N., Makkonen, U., Garmash, O., Wang, Y., Zha, Q., Paasonen, P., Bianchi, F.,
853   Sipilä, M., Ehn, M., Petäjä, T., Kerminen, V. M., Worsnop, D. R., and Kulmala, M.: The role
854   of H2SO4-NH3 anion clusters in ion-induced aerosol nucleation mechanisms in the boreal
855   forest, Atmos. Chem. Phys., 18, 13231-13243, 10.5194/acp-18-13231-2018, 2018.
856
857 Yang, D., Zhang, S., Niu, T., Wang, Y., Xu, H., Zhang, K. M., and Wu, Y.: High-resolution mapping
858   of vehicle emissions of atmospheric pollutants based on large-scale, real-world traffic
859   datasets, Atmos. Chem. Phys., 19, 8831-8843, 10.5194/acp-19-8831-2019, 2019.
860
861 Yao, L., Garmash, O., Bianchi, F., Zheng, J., Yan, C., Kontkanen, J., Junninen, H., Mazon, S. B.,
862   Ehn, M., Paasonen, P., Sipilä, M., Wang, M., Wang, X., Xiao, S., Chen, H., Lu, Y., Zhang,
863   B., Wang, D., Fu, Q., Geng, F., Li, L., Wang, H., Qiao, L., Yang, X., Chen, J., Kerminen, V.-
864   M., Petäjä, T., Worsnop, D. R., Kulmala, M., and Wang, L.: Atmospheric new particle
865   formation from sulphuric acid and amines in a Chinese megacity, Science, 361, 278-281,
866   10.1126/science.aao4839 2018.
867
868 Yao, L., Fan, X., Yan, C., Kurtén, T., Daellenbach, K. R., Wang, Y., Guo, Y., Li, C., Dada, L., Cai,
869   J., Jun, T. Y., Zha, Q., Du, W., Yu, M., Zheng, F., Zhou, Y., Chan, T., Shen, J., Kujansuu, J.
870   T., Kangasluoma, J., Jiang, J., Li, H., Wang, L., Worsnop, D. R., He, H., Petäjä, T.,
871   Kerminen, V.-M., Liu, Y., Chu, B., Kulmala, M., and Bianchi, F.: Enhanced atmospheric
872   gaseous sulphuric acid formation from non-photochemical processes in urban Beijing,
873   China, 2020, In Prep.
874
875 Zamora, M. L., Peng, J., Hu, M., Guo, S., Marrero-Ortiz, W., Shang, D., Zheng, J., Du, Z., Wu, Z.,
876   and Zhang, R.: Measurement of aerosol properties during wintertime in Beijing, Atmos.
877   Chem. Phys. Discuss., 2019, 1-15, 10.5194/acp-2019-308, 2019.
878
879 Zhang, W., Tong, S., Ge, M., An, J., Shi, Z., Hou, S., Xia, K., Qu, Y., Zhang, H., Chu, B., Sun, Y.,
880   and He, H.: Variations and sources of nitrous acid (HONO) during a severe pollution
881   episode in Beijing in winter 2016, Sci Total Environ, 648, 253-262,
882   https://doi.org/10.1016/j.scitotenv.2018.08.133, 2019.
883
884 Zhou, Y., Dada, L., Liu, Y., Fu, Y., Kangasluoma, J., Chan, T., Yan, C., Chu, B., Daellenbach, K. R.,
885   Bianchi, F., Kokkonen, T. V., Liu, Y., Kujansuu, J., Kerminen, V. M., Petäjä, T., Wang, L.,
886   Jiang, J., and Kulmala, M.: Variation of size-segregated particle number concentrations in
887   wintertime Beijing, Atmos. Chem. Phys., 20, 1201-1216, 10.5194/acp-20-1201-2020, 2020.
888
889